International Research Journal of Engineering and Technology (IRJET) e-ISSN: 2395-0056
Volume: 05 Issue: 10 | Oct 2018 www.irjet.net p-ISSN: 2395-0072

# COMPUTATIONAL FLUID DYMAMIC ANALYSIS NATURAL CONVECTION FLOW THROUGH SQUARE CAVITY

**HIMANSHU MEHTA [1], K.K.JAIN [2], POOJA TIWARI[3], SOURABH VISHWAKARMA[4]**

[1]*M.E. Scholar (Heat Power Engg.) S.R.I.T.Jabalpur,M.P., India,*
[2]*Associate Professor Mechanical Engg. Department, S.R.I.T. Jabalpur, M.P., India,*
[3]*Professor (Mechanical Engg. Department) S.R.I.T. Jabalpur, M.P., India,*
[4]*M.E. Scholar T.I.T. Bhopa , M.P., India.*

---------------------------------------------------------------------***---------------------------------------------------------------------

**Abstract -** In CFD approaches, the partial differential equations are converted into algebraic equations by discretization methods (i.e. finite difference, finite volume and finite element method). The algebraic equations are modified to incorporate boundary conditions. The large set of algebraic equations so obtained, is then solved by iterative numerical procedures to obtain the

Unknown flow variables like pressure, velocity, temperature etc. at all grid points in the domain of interest. The solution can then be visualized in the form of velocity vector plot, contour plots of pressure, temperature or any other derived quantity. Important engineering quantities like heat flux, drag force, lift force; pressure drop etc. can be calculated from the solution.

**Index Terms-** heat transfer, Computational Fluid Dynamics CFD, convection, Rayleigh number, Nusselt Number.

## 1. INTRODUCTION

### 1.1OVER VIEW-

The natural convection flow and heat transfer in rectangular enclosures are extensively Studied due to its diverse applications. In the vertical position enclosures can acts as insulation for doors and windows of buildings, air conditioning compartment of trains, industrial furnaces, chimney and many heat transfer equipments and in an inclined position it is used in skylights, roof windows, solar collector storage and many other solar applications.

The present study is concern with natural convection heat transfer in vertical enclosures. The vertical enclosures consist of two glass panels set in a frame and separated by a small space. The gap between the glass panels is filled with air since air acts as insulator and air being a transparent medium allows light to pass through it. The 2-D representation of vertical enclosures is shown in the figure (1).

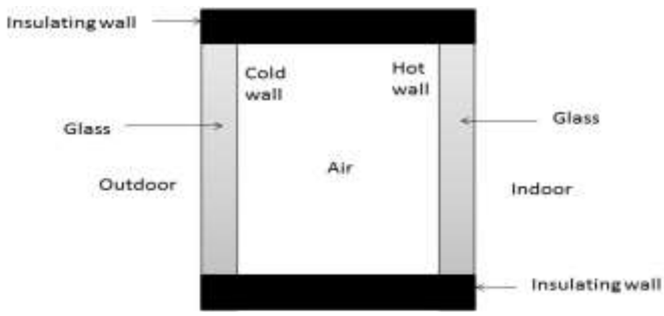


**Fig. 1 Two-dimensional representation of vertical enclosure**

The figure (1) shows vertical enclosures with two pieces of glass separated by a distance apart. In the present study a vertical enclosures is considered with side wall heating in which right wall is kept at a higher temperature and left wall is kept at lower temperature or vice-versa and top 2 and bottom walls are kept adiabatic. The space between two glass is filled with air to reduce the rate of heat transfer.

Heat transfer through vertical enclosures consists of following heat transfer mechanisms shown in figure (2):

1. Natural convection in the air trapped inside the enclosure.
2. Forced convection on the outdoor surfaces.
3. Conduction through the solid components of the glass.
4. Radiation from both the indoor and outdoor surfaces.

The present work is concerned with natural convection taking place inside vertical enclosures and neglecting the other modes of heat transfer.

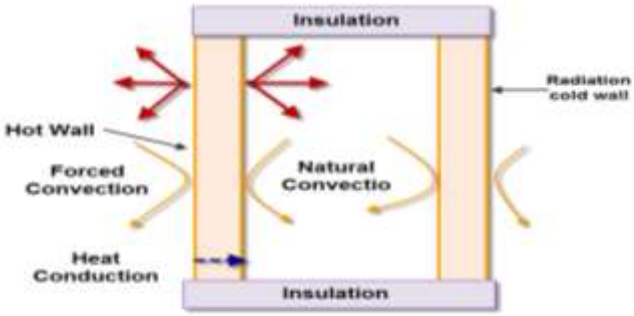


**Fig. 2 Modes of heat transfer in Vertical enclosure**

### 1.2 Dimensionless Parameters

**Nomenclature**

A = aspect ratio, H/L

g = acceleration due to gravity, $m/s^2$

H = height of the cavity, m

k = thermal conductivity of air, W/mK

L = width of the cavity

Nu = average Nusselt number for convective heat transfer across the cavity = $qL/k\Delta T$

Pr = Prandtl number of the fluid = $\boldsymbol{\nu/\alpha}$

P = pressure, Pa

q = average non radiative heat flow across air layer, $W/m^2$

Ra = Rayleigh number = $g\boldsymbol{\beta\Delta}TL^3/(\boldsymbol{\nu\alpha})$

Tc = temperature of cold wall, K

Th = temperature of hot wall. K

$\boldsymbol{\Delta}$T = temperature difference between the cold wall and the hot wall = Th − Tc, K

$\boldsymbol{\alpha}$ = thermal diffusivity of air, $m^2/s$

$\boldsymbol{\beta}$ = thermal expansion coefficient of air, K-1

$\boldsymbol{\nu}$ = kinematic viscosity of air, $m^2/s$

$\boldsymbol{\varphi}$ = angle of the glazing cavity from the horizontal

The problem considered here is that of a two-dimensional flow of a Boussinesq fluid. The geometry and boundary conditions of the flow region are shown in Figure. 1. The top and bottom walls are insulated i.e.

q(x,y=0) = 0

q(x,y=L) = 0

and the vertical walls are at constant temperatures,

T(x=0,y) = Tc

T(x=L,y) = Th

The components of velocity on the wall surfaces in both the x and y directions are

u(x=0,y) = v(x=0,y) = 0

u(x=L,y) = v(x=L,y) = 0

u(x,y=0) = v(x,y=0) = 0

u(x,y=L) = v(x,y=L) = 0

The following assumptions were made:

1. The Boussinesq approximation, which means, the variation in density is only important in the body force term of the governing equations.
2. An incompressible flow with negligible viscous dissipation.
3. Constant fluid properties.
4. No internal heat sources.

Fluid near the high temperature side will become hotter due to conduction and hence becomes less dense than the bulk fluid. A buoyancy force acting vertically upwards will develop resulting from the density difference. The less dense fluid near the higher temperature wall will rise. Similarly the fluid near the colder wall will fall because it is more dense than the surrounding fluid since it is at a lesser temperature than the bulk fluid. The result is a circulation pattern developing in a counter-clockwise manner if the right side wall temperature is larger than the left. Field Equations:

The convective heat transfer is governed by dimensionless parameters shown below:-

**Nusselt number (Nu):** The Nusselt Number at a surface within a fluid is the ratio of Convective heat to Conductive heat transfer across normal to the boundary.

$$\mathrm{Nu} = \frac{hL}{k} \qquad 1$$

**Rayleigh number (Ra):** The Rayleigh number is a measure determining the relative strength of conduction and convection. The Rayleigh number is product of Grashoff number (Gr) and Prandtl number (Pr)

$$Ra = \frac{g\beta \Delta T L^3}{v\alpha} \qquad 2$$

**Prandtl number (Pr) :** The Prandtl number (Pr) is the ratio of momentum diffusivity to thermal diffusivity. It provides a measure of relative effectiveness of the momentum and energy transport by diffusion.

$$Pr = \frac{v}{\alpha} \qquad 3$$

**Aspect ratio (A):** The Aspect ratio (A) is ratio of height of the cavity (H) to the length along

which heat transfer takes place.

$$A = \frac{H}{L} \qquad 4$$

### 1.3 Computational Fluid Dynamics (CFD)

Computational Fluid Dynamics CFD is a branch of fluid mechanics that uses numerical methods and algorithms to solve and analyze problems involving fluid flow, heat transfer, combustion etc. The governing equations (i.e. conservation of mass, conservation of momentum and conservation of energy) of fluid motion are usually described through fundamental mathematical equations (i.e. PDE partial differential equations).

A general form of partial differential equation which can represent various conservation laws of fluid flow is given below

**Continuity Equation**

$$\frac{\partial u}{\partial x} + \frac{\partial v}{\partial y} = 0 \qquad 5$$

**X-Momentum Equation**

$$\rho\left(u\frac{\partial u}{\partial x} + v\frac{\partial v}{\partial y}\right) = -\frac{\partial p}{\partial x} + \mu\left(\frac{\partial^2 u}{\partial x^2} + \frac{\partial^2 v}{\partial y^2}\right) \qquad 6$$

**Y- Momentum Equation**

$$\rho\left(u\frac{\partial u}{\partial x} + v\frac{\partial v}{\partial y}\right) = -\frac{\partial p}{\partial y} - \rho g\beta\Delta T + \mu\left(\frac{\partial^2 u}{\partial x^2} + \frac{\partial^2 v}{\partial y^2}\right) \qquad 7$$

**Energy Equation**

$$\rho C_p\left(u\frac{\partial T}{\partial x} + v\frac{\partial T}{\partial y}\right) = K\left(\frac{\partial^2 T}{\partial x^2} + \frac{\partial^2 T}{\partial y^2}\right) \qquad 8$$

In CFD approaches, the partial differential equations are converted into algebraic equations by discretization methods (i.e. finite difference, finite volume and finite element method). The algebraic equations are modified to incorporate boundary conditions. The large set of algebraic equations so obtained, is then solved by iterative numerical procedures to obtain the

Unknown flow variables like pressure, velocity, temperature etc. at all grid points in the domain of interest. The solution can then be visualized in the form of velocity vector plot, contour plots of pressure, temperature or any other derived quantity. Important engineering quantities like heat flux, drag force, lift force; pressure drop etc. can be calculated from the solution.

## 2. Objectives

- The objective of the present study is to employ CFD methodology for computing laminar natural convection flow and heat transfer in two-dimensional vertical air cavities.
- The Nusselt number is a function of Rayleigh number, Aspect ratio, Inclination and Prandtl number. In the present study the Prandtl number and inclination are constant so the Nusselt number is the function of Rayleigh number and Aspect ratios.
- In the present study Nusselt number is computed for steady, laminar natural convection in vertical enclosures using commercial Computational Fluid Dynamics code for wide range Rayleigh number varying $10^3 \le Ra \le 10^6$ and aspect ratios vary from 1 to 10 at the rate of 2.5.
- The details of flow features is studied with the help of stream function and temperature Distribution is studied to understand the heat transfer trends in vertical enclosures with side wall heating.
- In the present study Nu-Ra correlations are proposed for wide range Rayleigh number varying $10^3 \le Ra \le 10^6$.

## 3. Problem Identification

The present study deals with two-dimensional natural convection taking place inside enclosed Space. The enclosed cavity has differentially heated side walls and adiabatic top and bottom wall. In this problem the cavity is filled with air and the effect of conduction and radiation is neglected. The space between the enclosures is filled with air since air being transparent allows light rays to pass through it and also acts as insulator.

### 3.1 Assumptions

The following assumptions are made in the present work:

1. Flow is steady laminar natural convection.

2. Flow is two -dimensional.

3. The fluid properties are constant except that the variation of density with temperature is accounted for in the formulation of buoyancy term (Boussinesq approximation).

4. The effect of conduction and radiation effects are neglected.

### 3.2 Scope of Present Study

The scope of the present study is to employ CFD methodology for computing laminar natural Convection flow and heat transfer in two-dimensional vertical air cavities. The dimensionless Parameter i.e. Nusselt number depends upon Rayleigh number, Aspect ratio, Inclination and Prandtl number. In the present study the Prandtl number and inclination are fixed in all the cases so the Nusselt number is the function of Rayleigh number and Aspect ratios. In the present study the Nusselt number is computed for the range of Rayleigh number and Aspect ratios is vary from 1 to 10 with the increment of 2.5..

**Range of Parameters Investigated**

Rayleigh number = $10^3$,$10^4$, $10^5$, $10^6$

Aspect ratio A = 1,2.5, 5, 7.5, 10

**Inclination θ** = $90^0$

Prandtl number (Pr) = 0.7

### 4. METHODOLOGY

### 4.1 Simulation Set-up

This chapter deals with natural convection flow and heat transfer in differentially heated enclosures. The geometry of cavity is created using Ansys 15 software by using geometry generation workbench for different Rayleigh number varying from $10^3$ to $10^6$ and aspect ratio constant at 1.aspect ratio 1 means we are using the square geometry for analysis. The heat transfer analysis is carried out using Ansys (Fluent).

#### 4.1.1 Geometric Creation

The geometry of the enclosed space, meshing and boundary identification is carried out in Ansys software. The dimensions of the cavity are permit to cover wide range of Rayleigh number ($10^3 \le Ra \le 10^6$) and aspect ratio 1. The fig. 3 shows geometry of square enclosure for Ra=$10^3$.

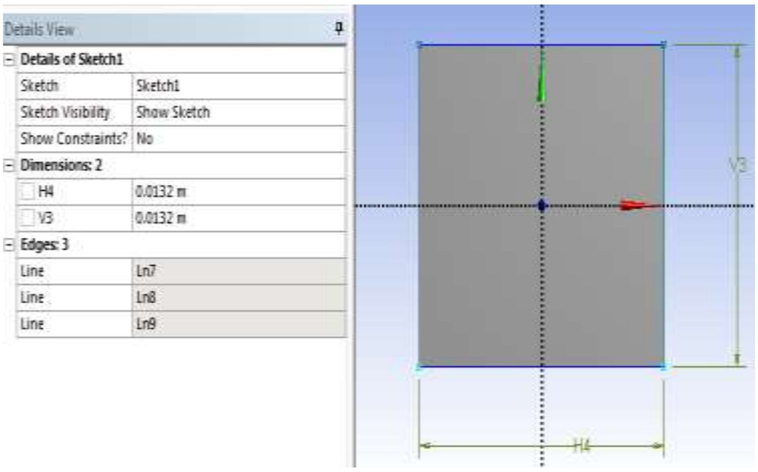


**Fig.3 Geometry of Square enclosed space for Ra=$10^3$**

The creation of geometry in ansys software is based on hierarchical order. It means that first Coordinates of the geometry are created and then curves are drawn through coordinates and finally face is created bounded by those curves. The face forms the computational domain. Similarly the geometry of other aspect ratio and Rayleigh no has been created in the same plate form and different dimension.

### 4.2 Dimensions of Cavities for Different Rayleigh Number

The dimensions of the length (L) of the cavity for different Rayleigh number varying from $10^3$ to $10^6$ is calculated by substituting the values of properties of fluid in the formula of Rayleigh Number. The height (H) of the cavity is found by multiplication of length (L) and aspect ratio (A) for a given Rayleigh number.

### 4.3 Mesh Generation

After creating the geometry it is required to divide the control volume into smaller number of Nodes and element of finite size, therefore it is called finite volume method. The method of splitting the Control volume into small finite size volume is known as meshing of the control volume. As Geometry is simple structured grid is preferred as it gives better results as compared to unstructured grid. Here we were using the minimum size of node 1e-04 m for mesh generation of square cavity.

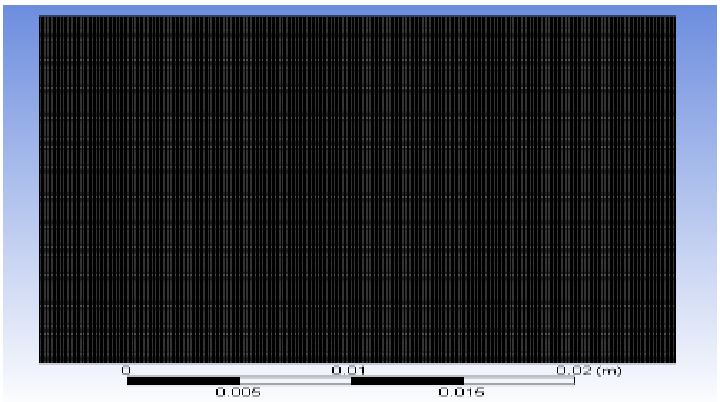


**Fig.4 meshing of Square enclosed space for Ra=$10^3$**

### 4.4 Selection of Scheme

i) Space - Two- Dimensional

ii) Solver - Pressure based

iii) Time - Steady

iv) Viscous - Laminar

v) Energy - On

vi) Gravity – On

### 4.5 Properties of Fluid

The properties of fluid are obtained at a mean temperature of differentially heated side walls, which is kept at temperature of $30^0$C and $35^0$C. The properties of air are calculated at $32.5^0$C.

**Table 1:- Properties of fluid air at $32.5^0$C**

| PROPERTY | UNIT | METHOD | VALUES |
|---|---|---|---|
| Temperature | K | Constant | 305.5 |
| Density | Kg/M3 | Boussinesq | 1.15575 |
| Specific heat | J/kgK | Constant | 1005 |
| Thermal conductivity | W/mk | Constant | 0.02634 |
| Viscosity | Kg/ms | Constant | 1.87E-05 |
| Thermal expansion | 1/K | Constant | 0.003273 |
| Gravitational acceleration | m/s2 | Constant | 9.801 |
| Dynamic viscosity | Kg/ms | Constant | 0.00002074 |
| Beta | 1/k | Constant | 2.87E-03 |

### 4.6 Boundary Condition

The enclosed cavity has differentially heated side walls and adiabatic top and bottom wall which is shown in table 2 below.

**Table 2 Boundary condition of square cavity**

| ***BOUNDARY*** | ***TYPE*** | ***VALUES*** |
|---|---|---|
| Side wall | Isothermal | T=308 K |
| Rigth wall | Isothermal | T=303 K |
| Top wall | Adiabatic | q= 0 W/m2 |
| Bottom wall | Adiabatic | q= 0 W/m2 |

### 4.7 Solution method

*1) In order to solve the given boundary condition in ansys fluent workbench we were using the Pressure-Velocity Coupling Method. ANSYS Fluent provides four segregated types of algorithms: SIMPLE, SIMPLEC, PISO, and (for time-dependant flows using the Non-Iterative Time Advancement option (NITA) Fractional Step (FSM). These schemes are referred to as the pressure-based segregated algorithm. Steady-state calculations will generally use SIMPLE or SIMPLEC, while PISO is recommended for transient calculations. PISO may also be useful for steady-state and transient calculations on highly skewed meshes. In ANSYS Fluent, using the Coupled algorithm enables full pressure-velocity coupling, hence it is referred to as the pressure-based coupled algorithm.*

### *2) 4.7.1 Spatial Discretization (SD)*

ANSYS uses a control-volume-based technique to convert the governing equations to algebraic equations that can be solved numerically. This control volume technique consists of integrating the governing equations about each control volume, yielding discrete equations that conserve each quantity on a control-volume basis.

Discretization of the governing equations can be illustrated most easily by considering the steady-state conservation equation for transport of a scalar quantity $\varphi$. This is demonstrated by the following equation written in integral form for an arbitrary control volume $v$ as follows:

$$\oint \rho\varphi \overline{v} \cdot d\overline{A} = \oint \Gamma_\varphi \nabla \varphi \cdot d\overline{A} + \int_V S_\varphi dV \qquad 9$$

Where

$\rho$ = density

$\tilde{V}$ = velocity vector

$\bar{A}$ = surface area vector

$\Gamma_\varphi$ = diffusion coefficient for $\varphi$

$\nabla\varphi$ = gradient of $\varphi$

$=(\frac{\partial\varphi}{\partial x})i\hat{} + (\frac{\partial\varphi}{\partial y})j\hat{}$ in 2D)

$S_\varphi$ = source of $\varphi$ per unit volume

### 4.7.2 Discretisation Scheme Used

i) Pressure velocity coupling - SIMPLE

ii) Pressure standard momentum - 2nd orders UPWIND

iii) Energy - 2nd order UPWIND

### 4.8 Convergence Criteria

The convergence criteria are set $10^{-3}$ for continuity, x-momentum, y-momentum and $10^{-6}$ for energy equation. The convergence is shown for square enclosures at $Ra=10^6$. It is observed that convergence criteria are satisfied for continuity, momentum and energy equation.

At the end of each solver iteration, the residual sum for each of the conserved variables is computed and stored, thereby recording the convergence history. This history is also saved in the data file. The residual sum is defined below.On a computer with infinite precision, these residuals will go to zero as the solution converges. On an actual computer, the residuals decay to some small value ("round-off") and then stop changing ("level out"). For single-precision computations (the default for workstations and most computers), residuals can drop as many as six orders of magnitude before hitting round-off. Double-precision residuals can drop up to twelve orders of magnitude.

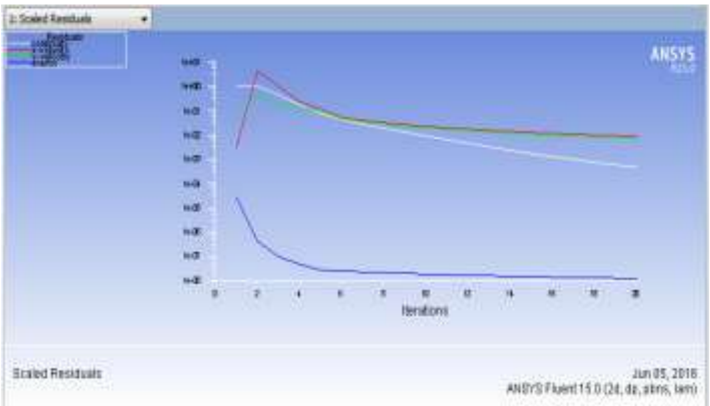


**Fig 5:- Convergence window of square enclosure at $Ra = 10^6$**

### 4.9 Post Processing

After convergence of solution, the flow pattern is visualized with help of contours of stream function and temperature contours. In the present study average Nusselt number is obtained using Ansys (Fluent) software which is the key parameter in natural convection heat transfer.

CFD-Post has the following features:

1. A graphical user interface that includes a viewer pane in which all graphical output from CFD-Post is plotted.
2. Support for a variety of graphical and geometric objects used to create post-processing plots, to visualize the mesh, and to define locations for quantitative calculation.
3. Scalar and vector user-defined variables.
4. Variable freezing (for comparison with other files)
5. Post-processing capability for turbo machinery applications.
6. Standard interactive viewer controls (rotate, zoom, pan, zoom box), multiple viewports, stored views/figures.
7. Extensive reports, including charting (XY, time plots)

## 5. RESULT & DISCUSSION

### 5.1 Validation of Present Results

In order to validate the code two-dimensional, laminar, steady natural convection of air with differentially heated side walls and adiabatic top and bottom walls of square cavity was solved. The thermal conditions and dimensions of the enclosures are permit to cover wide range of Rayleigh number varying from 103 to 106. The temperature difference between side walls was kept at constant for all the cases. The property of air is obtained at mean temperature of hot wall and cold wall. The computed results of heat transfer for average Nusselt number are obtained by using commercial Computational Fluid Dynamics software and compared with results available in the literature shown in the table 3.

**Table 3:- Validation of results for square enclousure**

| S No | Rayleigh Number Ra | Present Study (Nu) | Byong-Hoon Chang [1] (Nu) | De Vahl [8] (Nu) |
|---|---|---|---|---|
| 1 | $10^3$ | 1.17 | 1.118 | 1.118 |
| 2 | $10^4$ | 2.08 | 2.241 | 2.243 |
| 3 | $10^5$ | 4.48 | 4.532 | 4.519 |
| 4 | $10^6$ | 8.86 | 8.848 | 8.799 |

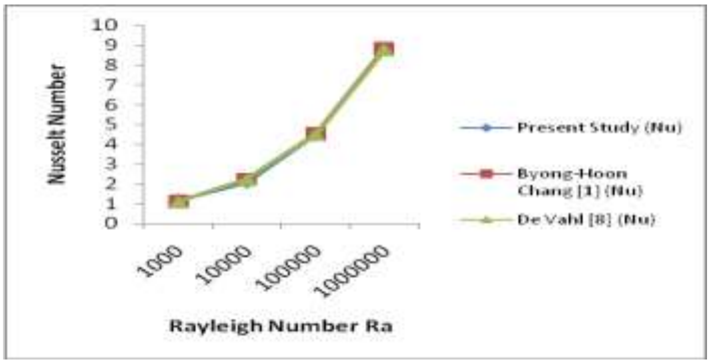


**Fig. 5.1: Validation of Nusselt number for square enclosure at different Rayleigh number**

**5.2 Result of Heat transfer for square cavity and different Rayleigh No.**

The computation fluid dynamic analysis in ansys fluent workbench has performed to find out the Nusselt number and natural convection or nature of heat transfer from hot medium to cold medium. In order to find out the result in ansys fluent we perform 200 iteration for each combination of aspect ratio and Rayleigh No. Fluent provide wide range of solution in terms of continuity, energy, and velocity in x and y direction with respect to the time. On the basis of each result we calculate the average nusselt number by maximum and minimum range by using user define function. The result tabulated below in table 4

**Table 4:- Nusselt number of Square cavity for different Rayleigh number**

| Rayleigh number | Nusselt Number (Nu) |
|---|---|
| $10^3$ | 1.17 |
| $10^4$ | 2.08 |
| $10^5$ | 4.48 |
| $10^6$ | 8.86 |

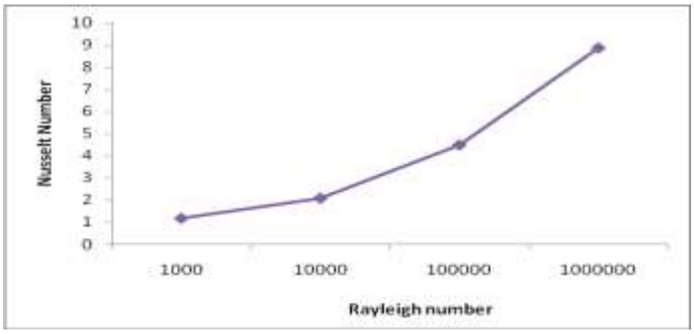


**Fig. 6: Variation of Nusselt number with Rayleigh number at A=1**

### 5.3 Stream Function Plot for Square Enclosure

The stream function plot is use to visualize the flow of air in square cavity for different Rayleigh number varying from $10^3$ to $10^6$ shown in fig.7

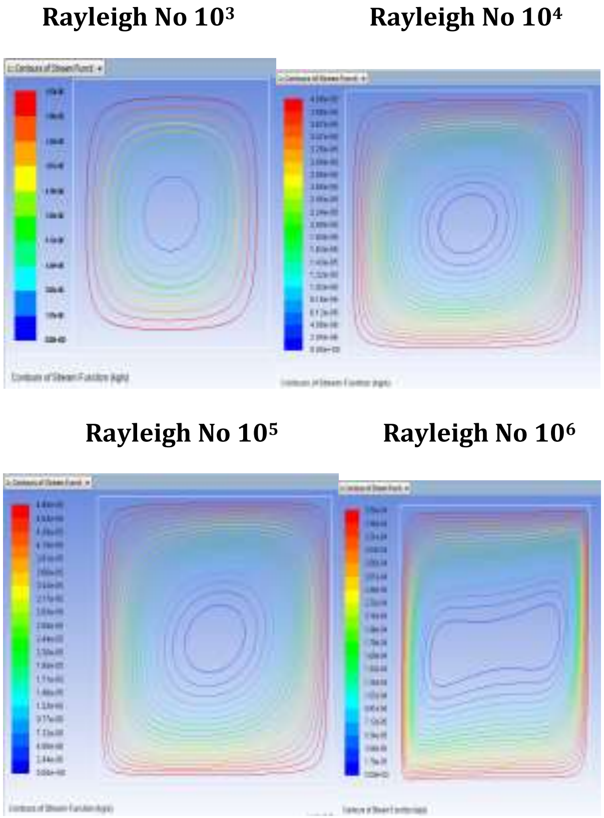


**Fig. 7: Stream function plot for square cavity at different Rayleigh number**

It is observed that for all Rayleigh number circulation of air takes place from upward to downward. The circulation pattern exists due to density difference between side walls maintained at different temperature. It is observed that flow is unicellular for $10^3 \leq Ra \leq 10^4$ and multi-cellular for $10^5 \leq Ra \leq 10^6$.

### 5.4 Temperature Contours for Square Cavity

The temperature contour plots is used to study temperature distribution of air in square enclosures for different Rayleigh number varying from $10^3$ to $10^6$ shown in the fig. 8 the detail study of temperature contour its is found that the path of contour becomes irregular with increasing the Rayleigh No.

### 5.5 Heat Transfer Correlations Proposed for Square Cavity

Based on present results of Nusselt number obtained by Computational Fluid Dynamics , the correlations of heat transfer is proposed using Least square curve Square cavity (i.e. A=1).

The proposed correlation for heat transfer is valid for small aspect ratio and lower Rayleigh Number. The proposed correlation for heat transfer is given by:

**$Nu=0.1225 (Ra)^{0.31}$……………………………eq. (10)**

Range of Parameters Investigated:-

Aspect Ratio (A=1).

Rayleigh number ($10^3 \leq Ra \leq 10^6$).

Inclination: ($\theta=90^0$)

### 5.6 Comparison of Proposed Correlation with the Result Obtained from CFD Analysis:

**Table 5:- Nusselt No. comparison between correlation and fluent result**

| Rayleigh number | Nusselt Number (Nu) (fluent analysis) | Nusselt Number (Nu) (correlation) | Percentage deviation in % |
|---|---|---|---|
| 1000 | 1.17 | 1.04 | 10.88% |
| 10000 | 2.08 | 2.13 | 2.34% |
| 100000 | 4.48 | 4.35 | 2.98% |
| 1000000 | 8.86 | 8.87 | 0.16% |

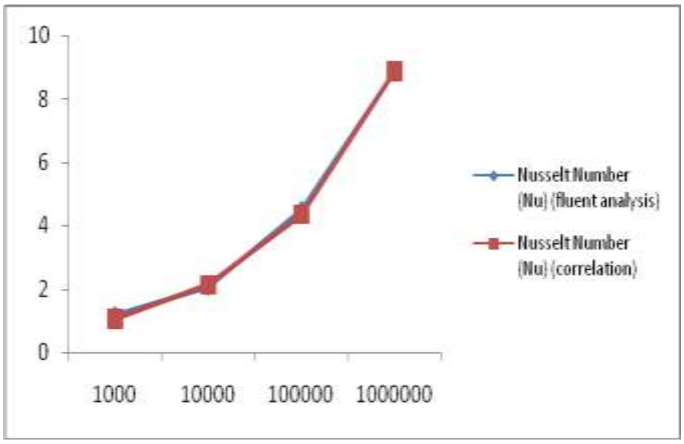


**Fig. 8: Nusselt No. comparison between correlation and fluent result**

It is observed that the present result of average Nusselt number computed from CFD fluent analysis shows very close agreement with the result obtained from the correlation suggested.

### 5.8 Results of Heat Transfer for Medium Aspect Ratio and Lower Rayleigh Number

The average Nusselt number for medium aspect ratios ($2.5 \leq A \leq 10$) and lower Rayleigh number ($10^3 \leq Ra \leq 10^6$) is computed using CFD code It is observed from table 6 that Nusselt number increases with increase in Rayleigh number and decreases with increases in Aspect ratios.

**Table 6:- Results of heat transfer at Ra=$10^3$ to $10^6$ and A= 1 to 10.**

| S.No. | Rayleigh Number (Ra) | Aspect ratio (A) | Nusselt Number (Nu) Present Work (2-D CFD) |
|---|---|---|---|
| 1 | $10^3$ | 2.5 | 1.14 |
| 2 | $10^3$ | 5 | 1.08 |
| 3 | $10^3$ | 7.5 | 1.06 |
| 4 | $10^3$ | 10 | 1.04 |
| 5 | $10^4$ | 2.5 | 2.25 |
| 6 | $10^4$ | 5 | 2.03 |
| 7 | $10^4$ | 7.5 | 1.82 |
| 8 | $10^4$ | 10 | 1.69 |
| 9 | $10^5$ | 2.5 | 4.18 |

| | | | |
|---|---|---|---|
| 10 | $10^5$ | 5 | 3.74 |
| 11 | $10^5$ | 7.5 | 3.45 |
| 12 | $10^5$ | 10 | 3.20 |
| 13 | $10^6$ | 2.5 | 7.60 |
| 14 | $10^6$ | 5 | 6.65 |
| 15 | $10^6$ | 7.5 | 6.21 |
| 16 | $10^6$ | 10 | 6.00 |

### 5.9 Stream Function Plot for Vertical Enclosure

The stream function plot is use to visualize the flow of air in vertical enclosures for different Rayleigh number varying from $10^3$ to $10^6$ and aspect ratios from 1 to 10. It is observed from figure (5.6) that for all aspect ratios circulation of air takes place from upward to downward. The circulation pattern exists due to density difference between side walls maintained at different temperature. It is seen that flow is unicellular for all aspect ratios.

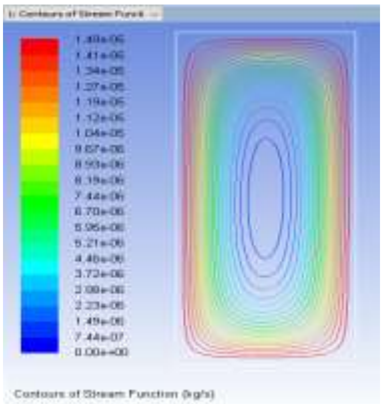


A = 2.5

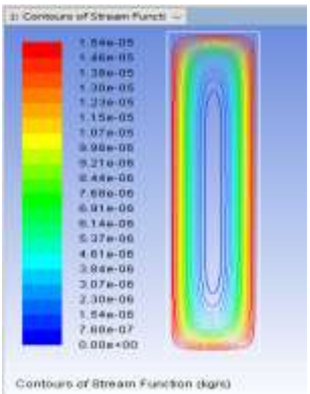


A = 5

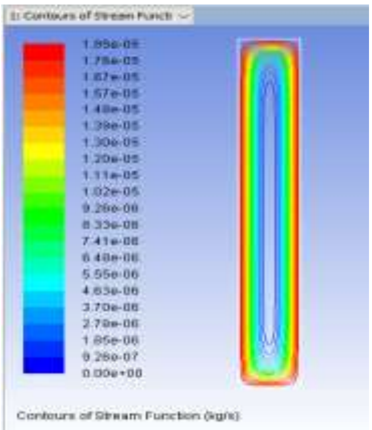


A = 7.5

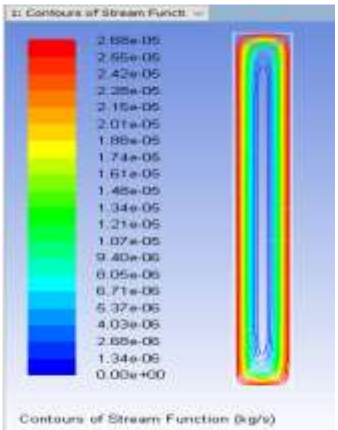


A = 10

**Fig. 9: Stream function plot for vertical enclosures at Ra = $10^3$ A=2.5, A=5, A=7.5 and A=10**

It is observed from figure 10 contours of stream function for vertical enclosures are unicellular for all aspect ratios. The flow pattern of air inside vertical enclosures at Rayleigh Number $10^4$ is similar to Rayleigh number $10^3$ but the magnitude of stream function increases with Rayleigh number.

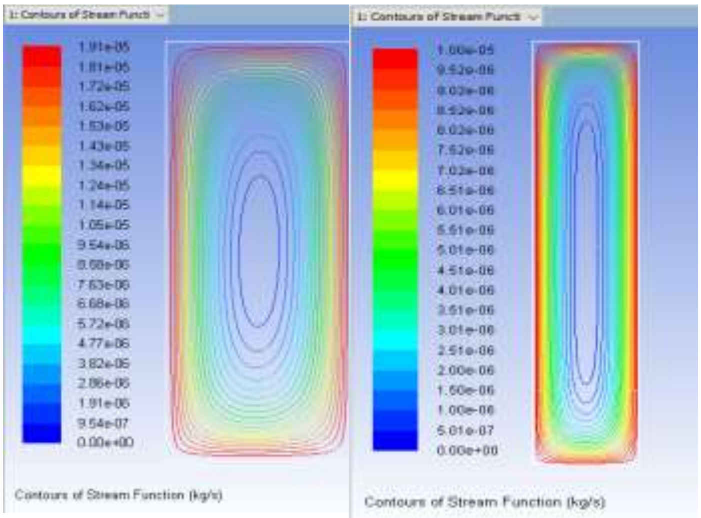


**A = 2.5** **A = 5**

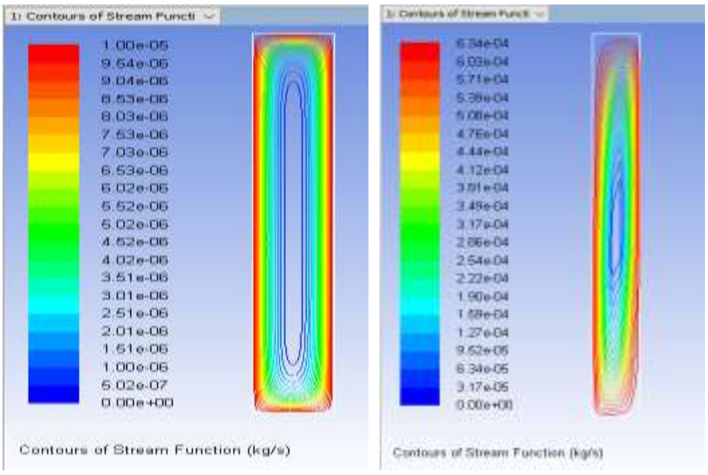


**A = 7.5** **A = 10**

**Fig. 10: Stream function plot for vertical enclosures at Ra = $10^4$ A=2.5, A=5, A=7.5 and A=10**

The contours of stream function for vertical enclosures is unicellular for all small aspect ratios and becomes multi-cellular at higher aspect ratios for Rayleigh number $10^5$ as shown in fig. 11. The flow pattern of air inside vertical enclosures at Rayleigh number $10^5$ is complex at higher aspect ratios. It is observed that value of stream functions increases with aspect ratios.

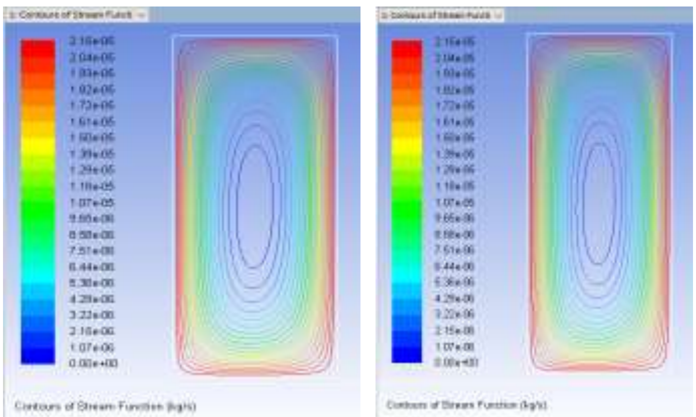

**A = 2.5** **A = 5**

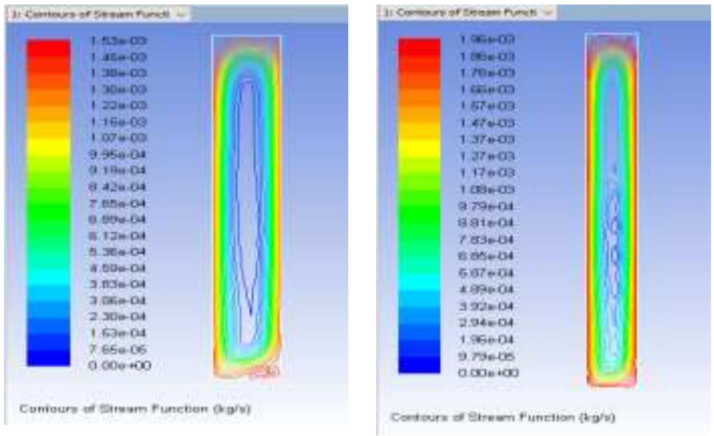


**A = 7.5** **A = 10**

**Fig. 11: Stream function plot for vertical enclosures at Ra = $10^5$ A=2.5, A=5, A=7.5 and A=10**

The contours of stream function for vertical enclosures is unicellular at Aspect ratio 2.5 and becomes multi-cellular at aspect ratios varying from 5 to 10 for Rayleigh number $10^6$ as shown in fig 12. The flow pattern of air inside vertical enclosures at Rayleigh number $10^5$ is very complex at all aspect ratios. It is observed that value of stream functions increases with aspect ratios.

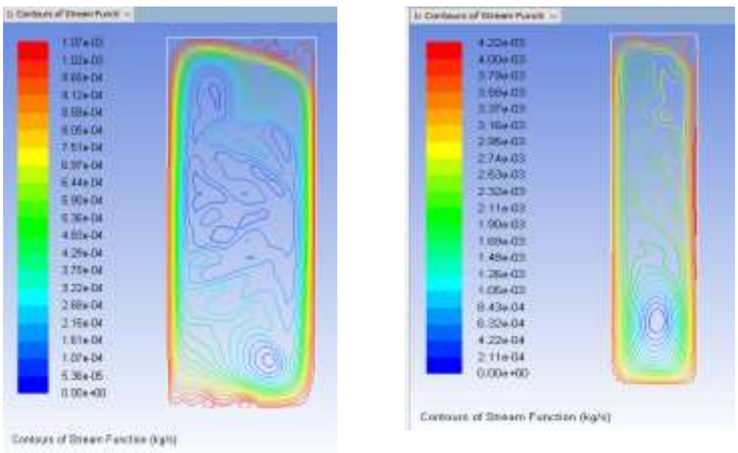


**A = 2.5** **A = 5**

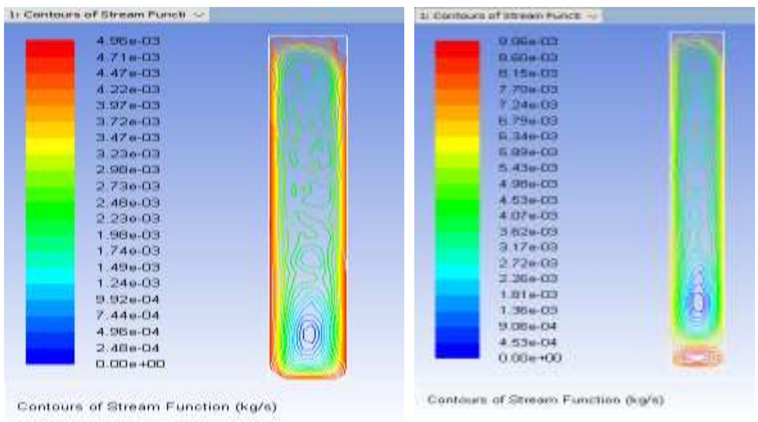


**A = 7.5** **A = 10**

**Fig. 12: Stream function plot for vertical enclosures at Ra = $10^5$ A=2.5, A=5, A=7.5 and A=10**

### 5.10 Comparison of Present Correlations for Medium Aspect Ratios and Lower Rayleigh Number

The present correlation for heat transfer in enclosed spaces for medium aspect ratios (2.5≤A≤10) and lower Rayleigh number ($10^3 \le Ra \le 10^6$) is validated with the correlations given by Byong-Hoon Chang [1] and is shown in table (12) to (15). The present correlations under predict the correlations given by Byong-Hoon Chang [1] and deviates by about 1 to 10 %. The deviations seems to be quite high but the heat transfer correlations are only best possible curvefit of large amount of data. The fig. 13 to 16 shows the variation of Nusselt number with Aspect ratio for different Rayleigh number i.e. $10^3$, $10^4$, $10^5$, $10^6$.

**Table 7:- Comparison of Present correlation at Ra=$10^3$ and A= 1 to 10**

| Aspect ratio (A) | Nusselt Number (Nu) Present Work | Nusselt Number (Nu) Byong-Hoon Chang [1] |
|---|---|---|
| **1** | **1.07** | **1.34** |
| **2.5** | **1.14** | **1.21** |
| **5** | **1.08** | **1.13** |
| **7.5** | **1.06** | **1.08** |
| **10** | **1.04** | **1.04** |

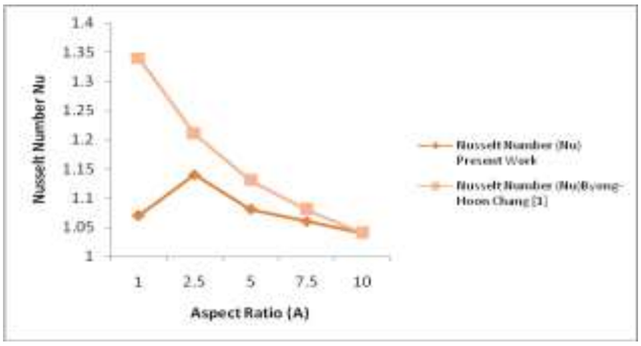


**Fig. 13:- Comparison of Present correlation for different aspect ratios at Ra=$10^3$**

**Table 8:- Comparison of Present correlation at Ra=$10^4$ and A= 1 to 10**

| Aspect ratio (A) | Nusselt Number (Nu) Present Work | Nusselt Number (Nu) yong-Hoon Chang [1] |
|---|---|---|
| 1 | 2.03 | 2.45 |
| 2.5 | 2.25 | 2.21 |
| 5 | 2.03 | 2.05 |
| 7.5 | 1.82 | 1.96 |
| 10 | 1.69 | 1.89 |

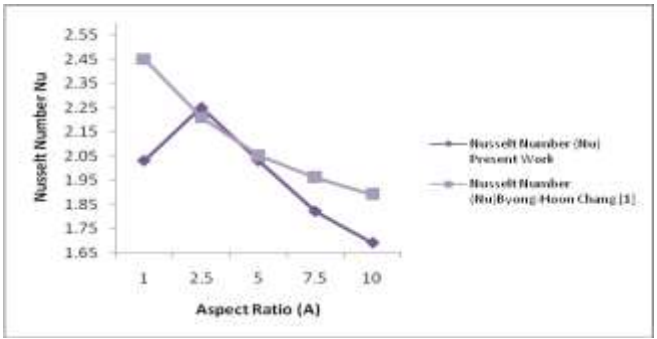


**Fig. 14:- Comparison of Present correlation for different aspect ratios at Ra=$10^4$**

**Table 9:- Comparison of Present correlation at Ra=$10^5$ and A= 1 to 10**

| Aspect ratio (A) | Nusselt Number (Nu) Present Work | Nusselt Number (Nu) Byong-Hoon Chang [1] |
|---|---|---|
| 1 | 4.52 | 4.44 |
| 2.5 | 4.18 | 4.02 |
| 5 | 3.74 | 3.73 |
| 7.5 | 3.45 | 3.56 |
| 10 | 3.2 | 3.45 |

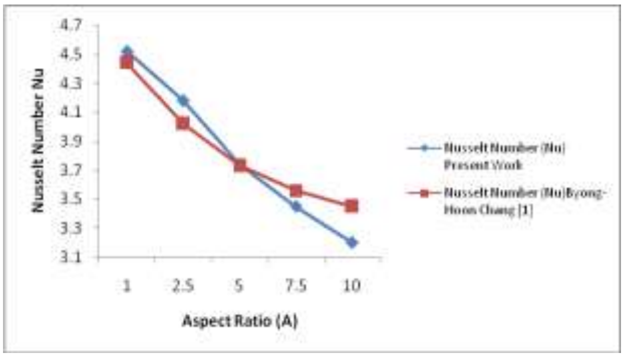


**Fig. 15:- Comparison of Present correlation for different aspect ratios at Ra=$10^5$**

**Table 10:- Comparison of Present correlation at Ra=$10^6$ and A= 1 to 10**

| Aspect ratio (A) | Nusselt Number (Nu) Present Work | Nusselt Number (Nu) Byong-Hoon Chang [1] |
|---|---|---|
| 1 | 8.89 | 8.1 |
| 2.5 | 7.6 | 7.32 |
| 5 | 6.65 | 6.78 |
| 7.5 | 6.21 | 6.49 |
| 10 | 6 | 6.28 |

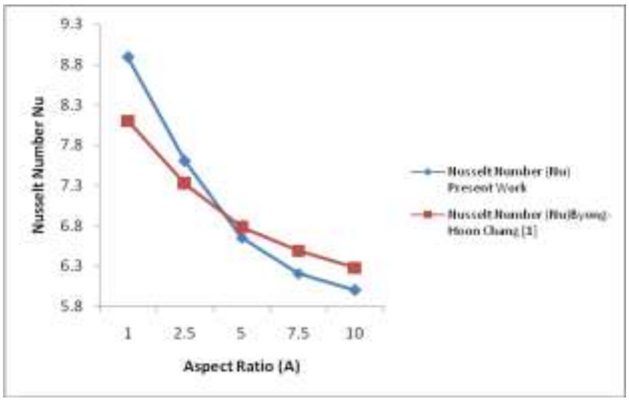


**Fig. 16:- Comparison of Present correlation for different aspect ratios at Ra=$10^6$**

## 6. CONCLUSIONS

The two different validation has been performed to analysed the nature of natural convection of heat transfer in square cavity. The phase I we compare the Fluent result with the results of Byong-Hoon Chang [1], and with reference to the graph plot in figure no 5.1 it shows that both curve are very close and reflect good agreement with each other. In second phase we compare the fluent result obtained by different aspect ratio of vertical cavity with correlation equation and it also show close relationship between both curves with reference to the table no. 5.4. So finally we concluded that the result obtained by the Computational fluid dynamic analysis of vertical cavity for different Rayleigh No. is close to the actual result.

The important conclusion can be summarized as follows:-

- It is observed that the Nusselt number increases with increase in Rayleigh number.
- It is investigated from stream function plot that for all Rayleigh number, circulation pattern exist and number of circulation cells increase with an increase in Rayleigh number.
- The temperature distribution of air inside enclosed spaces is obtained with the help of temperature contours.
- The present results of heat transfer for two-dimensional, laminar, steady natural convection flow is obtained by using Computational Fluid Dynamics Software and compared with the results of Byong-Hoon Chang [1]. The present results show very good agreement with results of Byong-Hoon Chang.
- Based on computational results of Nusselt number obtained by Computational Fluid Dynamics software, the correlations of heat transfer is proposed using least square curve fitting

for Small aspect ratio or square cavity and lower Rayleigh number.

$$\mathbf{Nu=0.1225\ (Ra)^{0.31}}$$

For Medium aspect ratios and lower Rayleigh number

$$\mathbf{Nu=0.23\ (Ra)^{0.2625}(A)^{-0.159}}$$

## 7. FUTURE SCOPE

- The present work is concerned with two-dimensional flow inside square enclosed space. The work can be further extended for three-dimensional Flow.
- In the present work air is used as working fluid. The work can be extended for different fluid.
- The present work is concerned with laminar natural convection flow. The work can be further extended for Turbulent Flow.
- In the present work the dependency of Rayleigh number is taken into consideration. The work can be further extended for varying aspect ratio, Prandtl number and inclinations of plate.
- In the present work the natural convection flow inside enclosed space is considered and the effect of radiation and conduction are neglected.
- The present work is concerned with aspect ratios one means for a square cavity. The work can be further extended for large Rayleigh number.
- The present work is concerned with vertical air cavity. The work can be further extended for various inclinations.

## 8. REFERENCES

a. Chang B.H. “Numerical Study of Flow and Heat Transfer in Differentially heated enclosures” International journal of Thermal Science, 18, 451-463, 2014.

b. Corcione, M., “Effects of the Thermal Boundary Conditions at the Sidewalls upon Natural Convection in Rectangular Enclosures Heated from Below and Cooled from Above”, International Journal of Thermal Sciences, 42, 199-208, 2003.

c. Elsherbiny S.M., Raithby G.D., Hollands K.G.T., “Heat transfer by natural convection across vertical and inclined air layers”, Journal of heat transfer, 1982, 104, 96-102.

d. Emery A.P., MacGregor R. K., “Free Convection through vertical plane layer: oderate and high Prandtl number fluids,” Journal of Heat Transfer, 91, 391, 1969.

e. F.P Incropera, D.P. Dewitt, Fundamental of heat and mass transfer. Fifth edition. Wiley India.

f. Fomichev, A., D.C. Curcija, B. Balagurunathan, and M. Stocki. . Investigation of heat transfer effects of sloped and ventilated internal cavities of framing systems, Final report.Amherst: Center for Energy Efficiency and Renewable Energy, University of Massachusetts,2007.

g. Fusegi, T., Hyun, J. M., and Kuwahara, K., “Natural Convection in a Differentially Heated Square Cavity with Internal Heat Generation,” Numerical Heat Transfer,1992, 21, 215–229.

h. G. De Vahl Davis, “ Natural convection of air in a square cavity: A bench mark numerical solution” International Journal for Numerical Methods in Fluids,3, 249–264,1983.

i. Henderson D., Junaidi H., Muneer T. Grassie T., Currie J., “Experimental and CFD investigation of an ICSSWH at various inclinations”, Renewable and Sustainable Energy Reviews, 11, 1087-1116, 2007.

j. Hollands K.G.T., Unny T.E., Raithby G.D., Konicek L., “Free convective heat transfer across inclined air layers”, Journal of heat transfer, 98, 189-193, 1976.

k. Hollands K.G.T., Konicek L., “Experimental study of the stability of differentially heated inclined air layers”, International Journal of Heat Mass Transfer, 16, 1467-1476, 1973.

l. Kothandaraman C.P., Subramanyan S., Heat and mass transfer data book., New Age International (P) limited.

m. Lage, J. L., and Bejan, A., “The Resonance of Natural Convection in an Enclosure Heated Periodically From the Side,” International Journal of Heat Mass Transfer, 36, 2027–2038,1993.

n. Lage, J. L., and Bejan, A, “The Ra-Pr Domain of Laminar Natural Convection in a Enclosure Heated From the Side,” Numerical Heat Transfer, 19, 21–41,1991.

o. Manz Heinrich., “Numerical simulation of heat transfer by natural convection in cavities of facade elements,” Energy and Buildings, 35,305–311, 2002.

p. Nogueria R.M., Martins.M.A.,Ampessan F0 .., “Natural convection in rectangular cavities with different aspect ratio”.Engenharia Termica (Thermal Engineering), 10,44-49,2011.

q. Ostrach, S., “Natural Convection in Enclosures,” ASME Journal of Heat Transfer,110,1175–1190,1988.

r. Ozoe, H., Sayma, H. and Churchill, S. W. “Natural Convection in an Inclined Rectangular Channel at Various Aspect Ratios and Angles-Experimental Measurements”, Int. J. Heat Mass Transfer, 18,1425-1431, 1975.

s. Pons Michel., “Transition from Single-to Multi-Cell Natural Convection of Air in Cavities with an Aspect Ratio of 20: A Thermodynamic Approach,” Int. J. of Thermodynamics, 11,71– 79, 2008.

t. Rajput R.K., “Textbook of Heat and Mass transfer”S. Chand & Company Ltd.

u. Soong, C. Y., “Numerical Study on Mode-Transition of Natural Convection in Differentially Heated Inclined Enclosure”, International Journal of Heat and Mass Transfer,,2869-2882, 1996.

v. Tian Y.S., Karayiannis T.G.., “Low turbulence natural convection in an air filled square cavity,” International Journal of Heat and Mass Transfer, 43,849–866, 1999.

w. Versteeg H.K., Malalasekera W. “Textbook of An introduction to computational fluid dynamics ” Longman Scientific and Technical.

x. Wenjiang Wu and Chan Y. Ching, “The Effect of the Top Wall Temperature on the Laminar Natural Convection in Rectangular Cavities With Different Aspect Ratios”, Journal of Heat Transfer ASME, , 131, 2009.